LETTER • OPEN ACCESS

Diverse impacts of sea ice and ice shelf melting on phytoplankton communities in the Cosmonaut Sea, East Antarctica

IOP Publishing Environ. Res. Lett. 20 (2025) 014003 https://doi.org/10.1088/1748-9326/ad975e

ENVIRONMENTAL RESEARCH
LETTERS

OPEN ACCESS

RECEIVED
9 August 2024

REVISED
16 November 2024

ACCEPTED FOR PUBLICATION
26 November 2024

PUBLISHED
6 December 2024

LETTER

Diverse impacts of sea ice and ice shelf melting on phytoplankton communities in the Cosmonaut Sea, East Antarctica

Qianqian Qi[1], Qiang Hao[2], Guang Yang[3], Shunan Cao[4,*], Jiawen Kang[1], Jiashun Hu[1], Minfang Zheng[1], Mengya Chen[1], Jianfeng He[4] and Min Chen[1,*]

[1] College of Ocean and Earth Sciences, Xiamen University, Xiamen 361102, People's Republic of China
[2] Second Institute of Oceanography, Ministry of Natural Resource, Hangzhou 310012, People's Republic of China
[3] Institute of Oceanology, Chinese Academy of Sciences, Qingdao 266000, People's Republic of China
[4] Polar Research Institute of China, Shanghai 201209, People's Republic of China
[*] Authors to whom any correspondence should be addressed.

E-mail: caoshunan@pric.org.cn and mchen@xmu.edu.cn

Keywords: sea ice, ice shelf, stable oxygen isotope, Bayesian isotope-mixing model, phytoplankton

Supplementary material for this article is available online

Abstract

Antarctic sea ice and glacier melt profoundly impacts marine ecosystems. Our study in the Cosmonaut Sea summer measures seawater oxygen isotopes, size-fractionated chlorophyll-a, and phytoplankton communities. We quantify sea ice meltwater, meteoric water, and winter water contents using a Bayesian isotope-mixing model. Contrary to common belief, our findings suggest that the reduced net export of sea ice to the north and the basal melting of ice shelves have deepened the mixed layer in coastal waters, altering the survival depth of phytoplankton. Freshwater primarily stimulates phytoplankton growth by supplying dissolved iron rather than by increasing water stability, which influences the size distribution and species composition of the phytoplankton community. These insights highlight the complex interplay between freshwater inputs, nutrient dynamics, and phytoplankton communities, and are crucial for understanding the dynamics of Antarctic ecosystem and its vulnerability to climate change.

1. Introduction

The Southern Ocean (SO) covers approximately 30% of the global ocean area and plays an important role in ocean circulation and the global climate system (Hyder *et al* 2018, Auger *et al* 2021). The SO accounts for more than 40% of anthropogenically derived carbon dioxide (CO_2) absorption and is the largest oceanic CO_2 sink (Sabine *et al* 2004, Landschützer *et al* 2015). Recent studies have shown that the amount of glacial meltwater (GMW) flowing into the ocean around Antarctica is increasing, linked to the calving of icebergs and basal melting of ice shelves (Pritchard *et al* 2012, Shepherd *et al* 2018). Freshening caused by GMW promotes ice shelf melting and inhibits the formation of Antarctic bottom water (Silvano *et al* 2018). Increased mass loss from the Antarctic ice sheet will become an important factor affecting sea level rise and the global overturning circulation (Rignot *et al* 2011, Silvano *et al* 2018). The SO overturning circulation controls the exchange of heat, carbon dioxide, and other properties between the deep ocean and the surface, significantly impacting the global biogeochemical cycling and climate. In addition to the ice shelves, sea ice cover in the SO also plays a vital role in the climate system by influencing global ocean circulation and ocean-atmosphere gas exchange. Sea ice forms at high latitudes and is exported northward via Ekman transport and ocean gyres. The brine released during sea ice formation contributes to the formation of dense shelf water (DSW), while the freshwater produced by sea ice melting facilitates the conversion of deep water into lighter mode water and intermediate water (Rintoul 2018). Therefore, the distribution of mean salinity in the SO is significantly influenced by freshwater transport by sea ice (Haumann *et al* 2016).

Dissolved iron and water stability are considered major factors regulating the growth of phytoplankton in the SO (Sambrotto *et al* 2003, Wang *et al* 2020).

Meteoric water (MW, including sources such as GMW and precipitation) and sea ice meltwater (SIM) are important sources of dissolved iron (Tamura *et al* 2023) and contribute to the formation of a stable and shallow mixed layer (Smith *et al* 2000, Sambrotto *et al* 2003, Behera *et al* 2020), thereby promoting phytoplankton growth. The temperature and salinity structures of the SO exhibit significant seasonal variation, with a shallower mixed layer in summer and a deeper mixed layer in winter. The change in mixed layer depth (MLD) between winter and summer forms a characteristic minimum temperature layer in the subsurface, known as winter water (WW), which represents the residual water from the previous winter's mixed layer. Above the WW lies the summer-warmed and fresher water, while below it is the relatively warmer circumpolar deep water (CDW) (Sabu *et al* 2020). Due to spatial variation in freshwater input, the salinity of WW varies across different sea areas. WW is crucial for the growth of phytoplankton in summer because it serves as a direct source of dissolved Fe for the upper ocean and contributes to the vertical stability of the water column (Sabu *et al* 2020).

The Cosmonaut Sea is located in East Antarctica, roughly between longitudes 30 °E and 65 °E and latitudes 60 °S and 68 °S. As a critical confluence point of the ACC, the Cosmonaut Sea borders Weddell-Enderby Land to the west, the Kerguelen Plateau to the north, and the Australian-Antarctic Basin to the east (Meijers *et al* 2010). Compared to other Antarctic waters, the Cosmonaut Sea is less studied, with its freshwater content previously unreported. In this study, we measured the oxygen isotope composition ($\delta^{18}O$), size-fractionated Chl *a* content, and phytoplankton community composition in the Cosmonaut Sea during summer. For the first time, we employed a Bayesian isotope mixing model to quantify the contents of SIM, MW, CDW, and WW based on $\delta^{18}O$ and salinity. We further elucidated the spatial variations of SIM, MW, CDW, and WW and their impacts on phytoplankton growth, which are crucial for assessing the effects of climate change on the Antarctic freshwater system and ecosystem.

2. Materials and methods

2.1. Sampling and analysis

Sample collection from the Cosmonaut Sea was conducted from 27 January to 11 March 2022, aboard the R/V *Xuelong 2*. Seawater samples from various depths at 52 stations were collected using a CTD-Rosette sampler for oxygen isotope ($\delta^{18}O$) analysis (figure 1). The sampling and analysis methods have been previously detailed (Brown *et al* 2014, Wang *et al* 2020). The size-fractionated Chl *a* concentrations were analyzed in three sequential steps: 20–200 μm (micro-Chl *a*), 2–20 μm (nano-Chl *a*), and 0.2–2 μm (pico-Chl *a*). Seawater was pre-filtered using a 200 μm mesh, followed by sequential filtration through 20 μm, 2 μm, and 0.2 μm pore size filters. Detailed information on the analytical procedures can be found in previous publications (Welschmeyer 1994). Seawater samples were collected and fixed with neutralized formaldehyde (final concentration of 5%) to determine the composition and abundance of phytoplankton communities. Phytoplankton was identified and enumerated using a flow imaging system (FlowCam, Fluid Imaging Technologies Inc., Yarmouth, ME). Seawater temperature and salinity were measured on-site using a Seabird 911-Plus CTD (Seabird, USA) with accuracies of $\pm$0.001 °C and $\pm$0.003 S/m, respectively. The MLD was determined by the depth of the maximum buoyancy frequency (Li *et al* 2024).

2.2. Calculation of water content from various sources

The $\delta^{18}O$ in seawater at high latitudes enables the separation and quantification of freshwater sources from sea-ice melt and meteoric origins (glacial melt and precipitation, Jia *et al* 2022). Previous studies have employed a three-end member mixing model of $\delta^{18}O$ and salinity to estimate the proportions of SIM, MW, and CDW (Meredith *et al* 2010, Wang *et al* 2020). Surface water is considered a mixture of CDW, SIM and MW, making it impossible to determine the content of WW, thereby affecting the understanding of WW structure and characteristics. Here, we innovatively apply a Bayesian isotope mixing model (Stable Isotope Analysis in R, SIAR; Parnell *et al* 2010) to simultaneously estimate the relative contributions of SIM, MW, WW, and CDW. The SIAR model utilizes a Bayesian framework to establish a logical prior distribution based on the Dirichlet distribution, enabling the calculation of source contributions (Evans *et al* 2000). This model provides possible distributions rather than definitive solutions for the relative contributions of multiple sources, thus allowing for the estimation of contributions from four sources using $\delta^{18}O$ and salinity. To accurately assess the contributions of the four sources, the characteristic values of SIM, MW, CDW, and WW were determined based on measurements and literature reports (Morgan 1972, 1982, Moore *et al* 2017, Jia *et al* 2022), as shown in table 1. The results of the calculation represent the Bayesian 95% credible intervals.

3. Results

3.1. Hydrographic properties

As illustrated in figure 1, the Cosmonaut Sea is primarily influenced by three major currents: the ACC, the Weddell Gyre, and the Antarctic Slope Current (Meijers *et al* 2010). The poleward boundary of the 1.5 °C isotherm in the upper CDW marks the

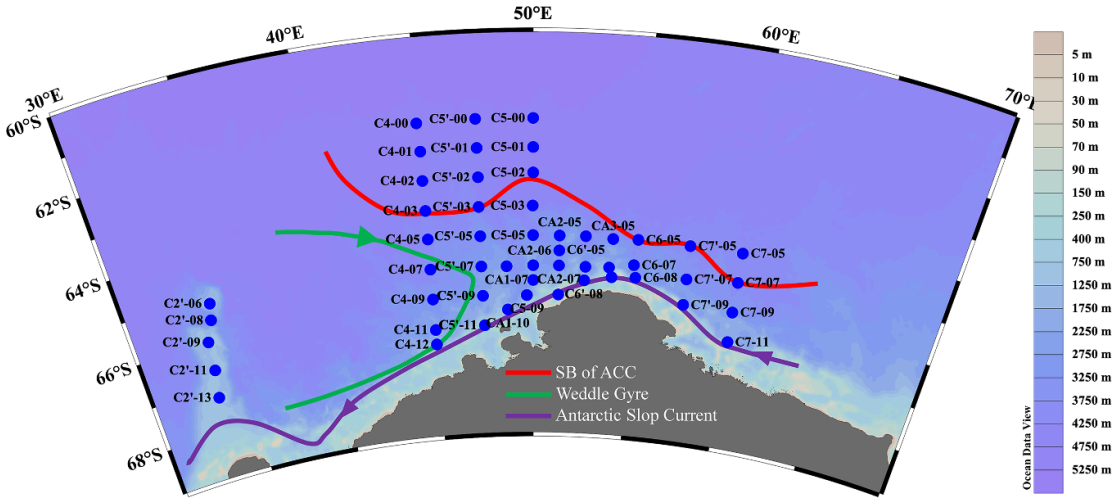

Figure 1. Sampling locations and major currents in the Cosmonaut Sea.

Table 1. Salinity and δ^{18}O characteristic values of the four end members in the Cosmonaut Sea.

End member	Salinity (psu)	δ^{18}O (‰)
SIM	6.000 ± 2.000	1.99 ± 0.15
MW	0.000 ± 0.000	–23.87 ± 9.67
CDW	34.713 ± 0.008	–0.05 ± 0.10
WW	34.236 ± 0.075	–0.50 ± 0.17

southern boundary (SB) of the ACC, which represents the southernmost extent of the upper overturning circulation (Orsi *et al* 1995, Yamazaki *et al* 2020). In this study, the position of SB was defined as the poleward limit of the 1.5 °C isotherm (figure 1). The influence of the Weddell Gyre is evident in the potential temperature and salinity properties of sections C4 and C5′, where the modified circumpolar deep water (MCDW) is notably warmer and saltier than in areas further east.

The distribution of potential temperature, salinity, and δ^{18}O in sections C2′, C5′ and C7 in the Cosmonaut Sea (Qi 2024) is shown in figure S1. The upper water column is dominated by Antarctic surface water (AASW) and WW, both characterized by lower salinity, potential temperature and δ^{18}O values. At depths greater than 200 m, saline, warm, and high-δ^{18}O CDW (including UCDW and LCDW) prevails. The distribution of the fractions of SIM, MW, WW, and CDW in sections C2′, C5′ and C7 is shown in figure S2. The contents of these source waters are very similar among the three sections. SIM and MW are mainly distributed within the upper 100 m, except for stations C5′-11 and C5′-09 on the shelf. The high MW contents observed in the deeper layers may be related to the basal melting of the ice shelf.

3.2. Spatial variation of SIM, MW and WW

The integrated content of SIM in the Cosmonaut Sea averages 0.89 m above 200 m and 1.13 m above 500 m. The average values of integrated MW content above 200 m and 500 m are 1.82 m and 2.32 m, respectively. High SIM and MW contents are observed in coastal waters and north of the SB, whereas low values are found near the SB and the Weddell Gyre (figure 2). Lower SIM, MW, and WW contents are observed between 64 °S and 66 °S (figure 2), likely linked to the upwelling near the SB of the ACC. The SB marks the southernmost reach of the Antarctic upper overturning circulation, where upwelling brings warm, salty deep water (i.e. CDW) to shallower layers (Yamazaki *et al* 2021). The impact of CDW upwelling in the Cosmonaut Sea is evidenced by positive anomalies in potential temperature and salinity at 200 m depth (figure S3) and sectional distributions of potential temperature and salinity (figure S1). This upwelling coincides with lower contents of SIM, MW, and WW, indicating that CDW upwelling reduces freshwater components in the upwelling core. The upwelled water partially moves northward at the surface, driven by prevailing westerly winds (Anderson *et al* 2009), pushing sea ice and icebergs northward. Additionally, the spatial variability of freshwater components in the Cosmonaut Sea is influenced by the Weddell Gyre, which transports water with low SIM and MW southward, creating a low-value area centered at ∼40 °E (figure 2).

Two primary mechanisms contribute to the loss of Antarctic ice shelves: atmospherically driven surface melting of glaciers and ocean-driven basal melting of ice shelves due to the upwelling of warm water onto the continental shelf (Banwell 2017, Lenaerts *et al* 2017). The ice shelves in the Cosmonaut Sea in East Antarctica are smaller and have been less studied (Pritchard *et al* 2012). Our study reveals that basal melting of ice shelves plays a crucial role in the spatial distribution of MW in the Cosmonaut Sea. On the continental shelf, the integrated content of MW above 200 m is significantly lower than

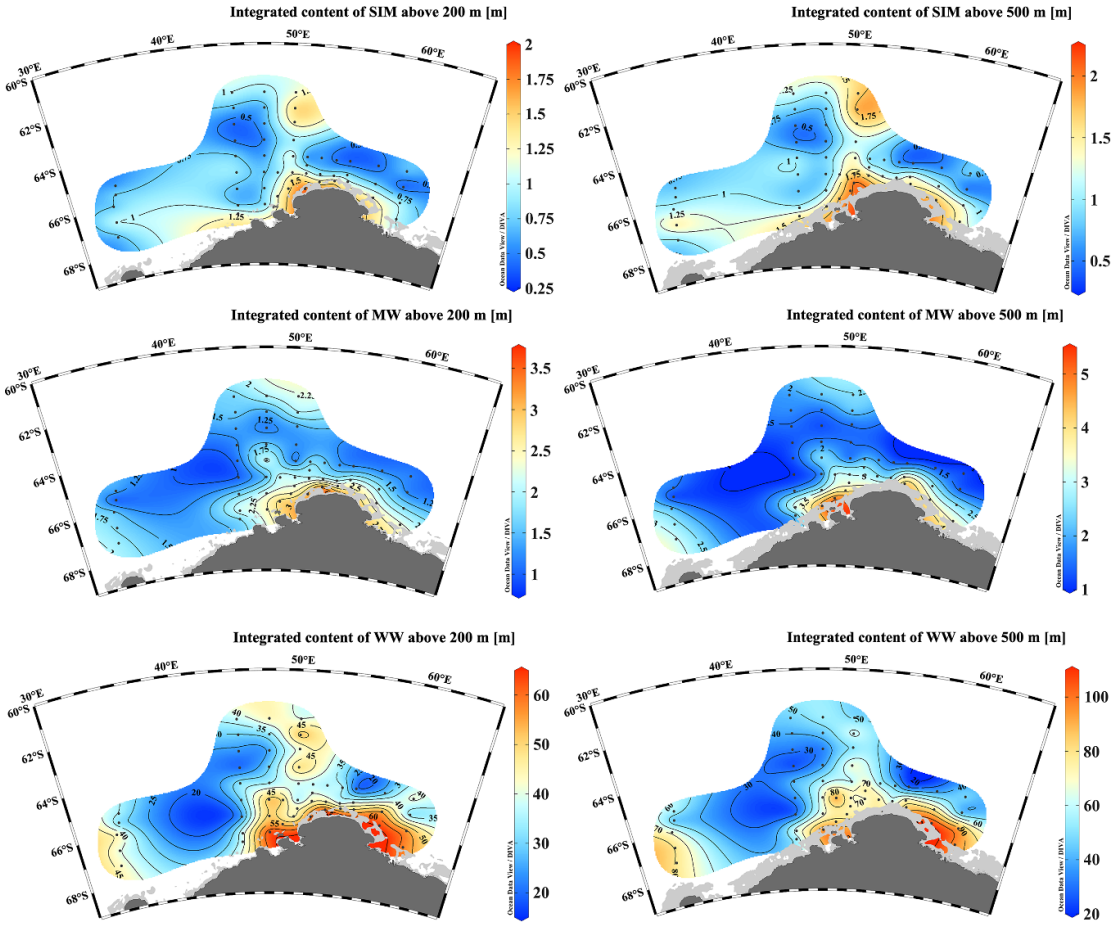

Figure 2. Spatial distribution of integrated contents of sea ice meltwater, meteoric water, and winter water above 200 m (left) and above 500 m (right) in the Cosmonaut Sea.

above 500 m, whereas, in the open sea, the integrated content above 200 m is similar to that above 500 m (figure 2). This suggests that water at depths of 200–500 m on the continental shelf is significantly impacted by the basal melting of ice shelves. The MW distribution along the coastal section also clearly shows substantial MW presence in the water layer below 200 m (figure 3). Therefore, we propose that basal melting of ice shelves, induced by MCDW intrusion, is a significant factor contributing to glacier loss in the Cosmonaut Sea. Minowa *et al* (2021) conducted direct measurements of ocean properties beneath the Langhovde Glacier ice shelf in the Cosmonaut Sea, and their results support our findings.

3.3. Spatial variation of phytoplankton

The average integrated contents of micro-Chl *a*, nano-Chl *a*, pico-Chl *a*, and total Chl *a* above 200 m were 30.55, 6.87, 6.17, and 43.59 mg m^{-2}, respectively. On average, micro-Chl *a* constituted approximately 70% of the total Chl *a*. Elevated levels of Chl *a* were detected in coastal waters (figure S4), which also exhibited high contents of SIM and MW (figure 2). The distribution of Chl *a* along the coastal section contrasted with salinity (figure 3), implying the influence of freshwater input (section 4.1). To examine the effects of freshwater components and WW on phytoplankton growth, we analyzed the relationships among the integrated contents of SIM, MW, WW, and Chl *a* above 200 m in the Cosmonaut Sea (table 2, figure S5). Significant correlations were observed between total Chl *a* and the integrated contents of SIM, MW, and WW, indicating that these factors significantly influence phytoplankton growth. SIM and WW were significantly correlated with micro-phytoplankton (20–200 μm) and nano-phytoplankton (2–20 μm), but not with pico-phytoplankton (<2 μm). MW content showed a strong positive correlation with Chl *a* across all three sizes. Our results suggest that SIM and MW are more conducive to the growth of larger phytoplankton (micro-phytoplankton and nano-phytoplankton, table 2 and figure S5). However, no significant relationship was found between freshwater and the percentage of micro-phytoplankton (figures 4(a) and (b)), indicating the variation in biomass and the percentage of micro-phytoplankton are different.

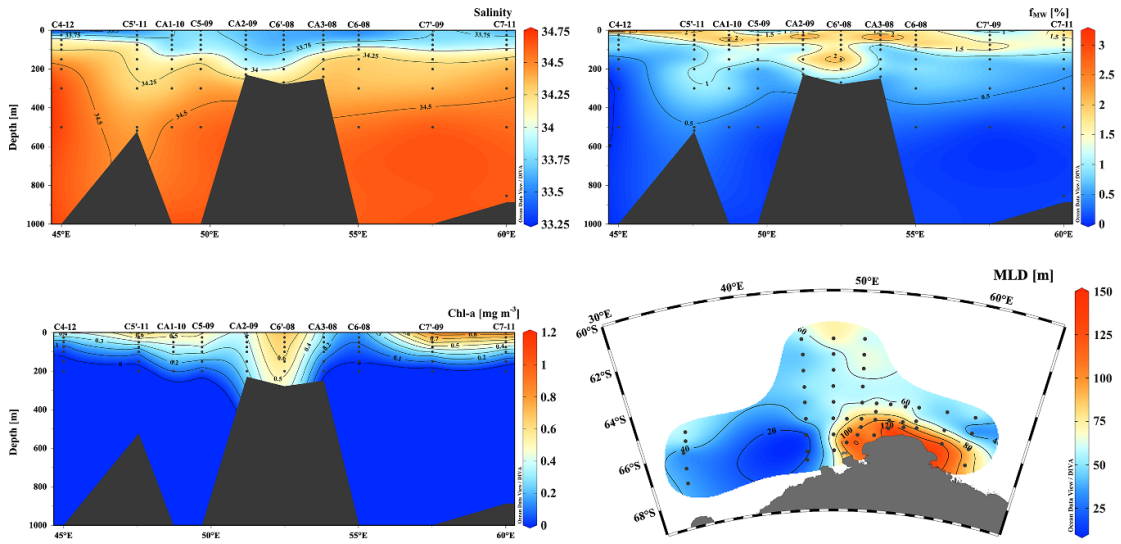

Figure 3. Distribution of salinity, meteoric water and Chl *a* along the coastal section and MLD in the Cosmonaut Sea.

Table 2. Correlations among sea ice meltwater (SIM), meteoric water (MW), winter water (WW), and Chl a in the Cosmonaut Sea.

	Chl *a*-Micro (mg m^{-2})	Chl *a*-Nano (mg m^{-2})	Chl *a*-Pico (mg m^{-2})	Total Chl *a* (mg m^{-2})
I_{SIM} (m)	0.429[a]	0.449[a]	0.214	0.442[a]
I_{MW} (m)	0.604[a]	0.622[a]	0.389[a]	0.631[a]
I_{WW} (m)	0.461[a]	0.463[a]	0.247	0.475[a]

[a] Correlation is significant at the 0.01 level ($P < 0.01$). I_{SIM}: integrated content of SIM above 200 m; I_{MW}: integrated content of MW above 200 m; I_{WW}: integrated content of WW above 200 m; Chl *a*-Micro: integrated content of micro-phytoplankton (20–200 μm) above 200 m; Chl *a*-Nano: integrated content of nano-phytoplankton (2–20 μm) above 200 m; Chl *a*-Pico: integrated content of pico-phytoplankton (0.2–2 μm) above 200 m.

The size of phytoplankton varies not only by group but also by growth phase (Shields and Smith 2009). The same phytoplankton group can contain species of different sizes (West *et al* 2024). We identified and counted more than one hundred phytoplankton species from three phyla (Bacillariophyta, Chrysophyta, and Pyrrophyta) at 17 stations. Bacillariophyta (diatoms) and Chrysophyta dominated the Cosmonaut Sea, comprising over 90% of the total biomass (figure S6). On average, Chrysophyta accounted for more than 60% of the total phytoplankton biomass. Within Chrysophyta, two species were identified: *Distephanus speculum* and *Phaeocystis sp.*, with *Phaeocystis sp.* being the dominant species (>99%). To further investigate the effects of freshwater on phytoplankton community structure, we analyzed the relationship between freshwater and the proportions of Bacillariophyta and *Phaeocystis sp.*, as illustrated in figures 4(c)–(f). SIM content was significantly positively correlated with the fraction of Bacillariophyta and negatively correlated with the fraction of *Phaeocystis sp.* In contrast, MW content showed no significant correlation with the proportion of Bacillariophyta and *Phaeocystis sp.* (figures 4(e)–(f)).

4. Discussions

4.1. The impact of freshwater on phytoplankton distribution

It is widely believed that SIM and MW promote the growth of phytoplankton by increasing water stability and providing iron (Sambrotto *et al* 2003, Behera *et al* 2020, Wang *et al* 2020, Tamura *et al* 2023). However, our study found that freshwater input triggered a deeper MLD in the Cosmonaut Sea, contradicting previously studies. Analyzing the causes of this phenomenon can enhance our understanding of the mechanisms by which SIM and MW affect phytoplankton growth.

The Antarctic continental shelf exhibits the highest rate of sea ice formation. The formed sea ice is transported northward by ocean gyres and Ekman transport, then melts at lower latitudes. Therefore, the continental shelf is the source area of sea ice, while lower latitude regions act as sinks (Rintoul 2018). For instance, the SIM content in the Amundsen Sea (Biddle *et al* 2019, Jeon *et al* 2021) and Prydz Bay (Jia *et al* 2022) gradually increases from nearshore to offshore, indicating that sea ice is exported from coastal areas. Contrary to these typical scenarios, sea

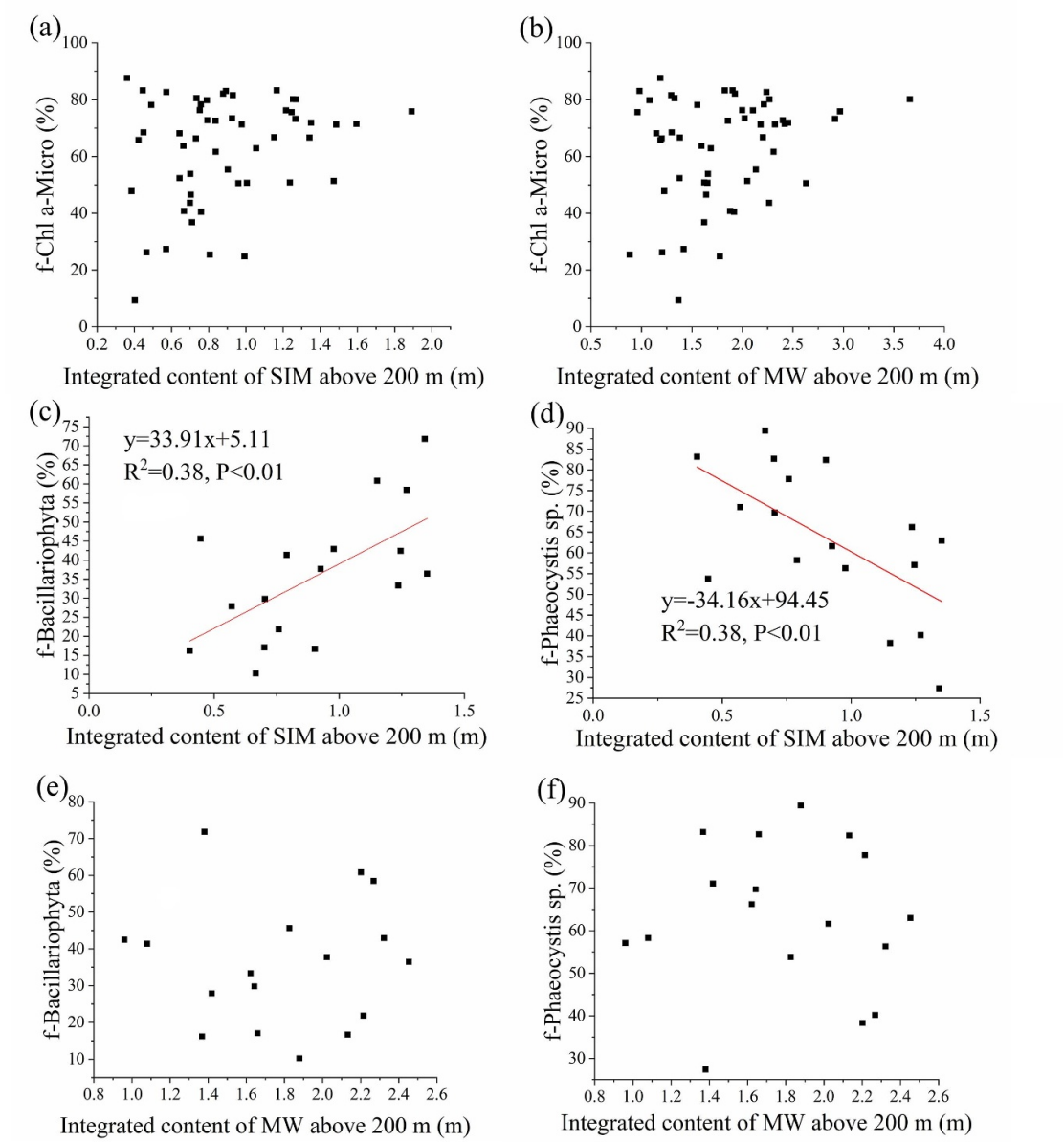

Figure 4. Relationship between SIM, MW contents, and fractions of micro-Chl *a* and various phytoplankton groups in the Cosmonaut Sea.

ice melt in the Cosmonaut Sea is mainly concentrated in the nearshore area to the edge of the continental shelf (figures 2 and 5). Additionally, the salinity of the shelf water in the Cosmonaut Sea is below 34.5 (figure 3), indicating minimal net brine rejection due to sea ice formation and export. This indicates that only a small amount of sea ice is exported from the continental shelf to the open ocean in the Cosmonaut Sea (figure 5).

The integrated MW content in the upper 500 m near the Pine Island Ice Shelf is approximately 10 m (Biddle *et al* 2019), which is twice the amount observed in the Cosmonaut Sea. Despite this, it still significantly impacts the ecosystem in this study. Generally, surface freshwater inputs in summer promote stratification of the water column (Smith *et al* 2000, Sambrotto *et al* 2003, Behera *et al* 2020), due to denser bottom water (figures 5(a) and (b)). However, in the Cosmonaut Sea, basal melting and reduced net brine rejection lower the salinity of the deep shelf waters (figure 5(c)), resulting in a smaller density difference in the water column. Previous studies have found that freshening caused by basal melting reduces DSW formation (figure 5(b), Williams *et al* 2016, Silvano *et al* 2018). In our study, basal melting of the ice shelf and low sea ice export lead to a deeper MLD on the shelf (figure 5), which may reduce light availability for phytoplankton in the water column. This observation aligns with the previously suggested plume theory. Basal melting near the grounding line produces a buoyant plume that upwells along the ice–ocean interface towards the open ocean (Minowa *et al*

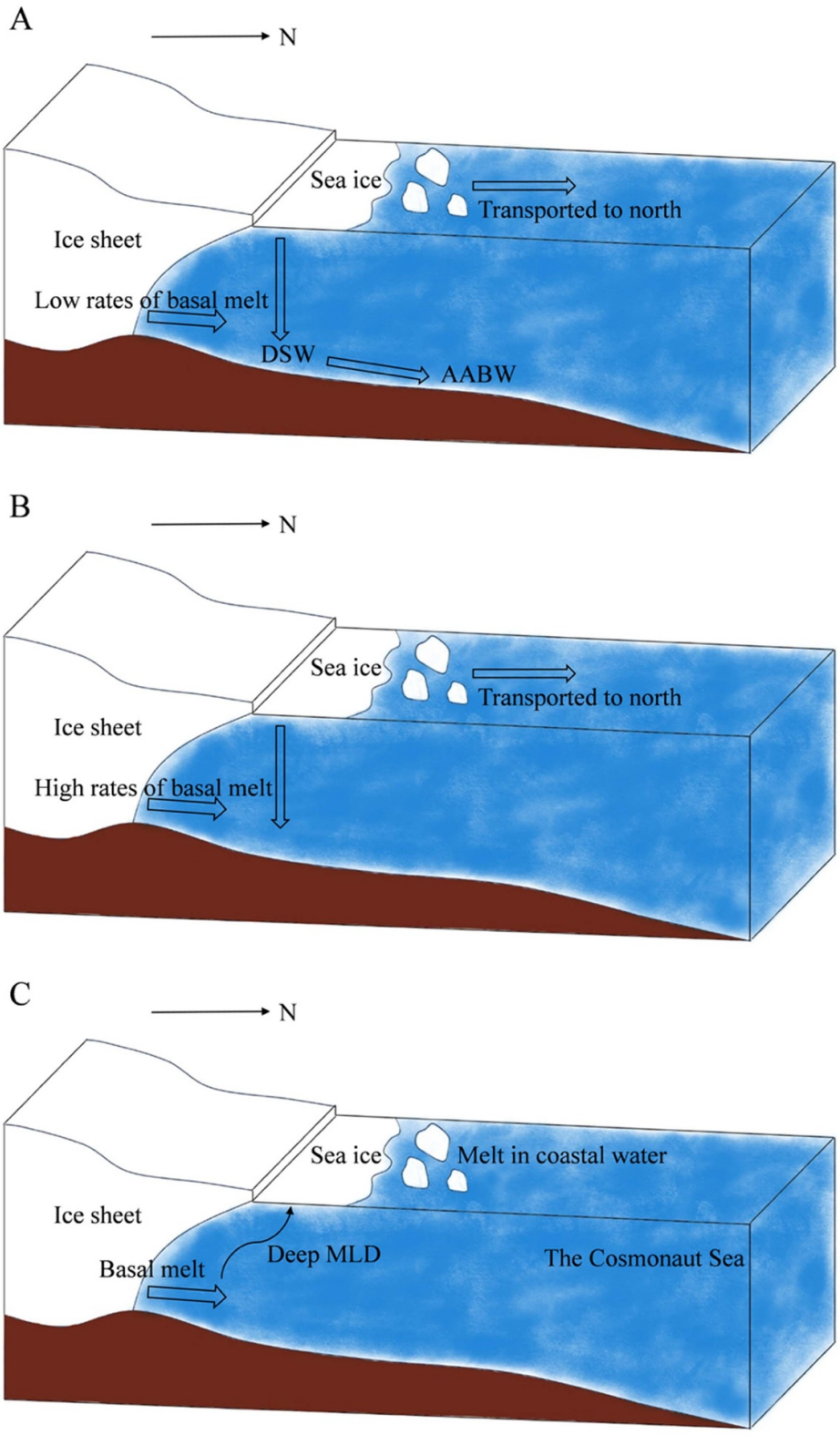

Figure 5. Impact of basal melting of ice shelf and sea ice transport on dense water formation and shelf stratification. (A) The ice shelf cavities are filled with cold shelf waters, resulting in low basal melt rates. The influx of glacial meltwater is insufficient to inhibit winter convection downstream of the meltwater outflow, thereby permitting the formation of dense shelf water, a precursor to Antarctic bottom water. (B) Modified circumpolar deep water induces rapid basal melting of the ice shelf. The substantial volume of glacial meltwater inhibits dense shelf water formation downstream of the meltwater outflow. (C) In the Cosmonaut Sea, low sea ice export prevents the formation of dense shelf water on the shelf. Basal melting of the ice shelf reduces the salinity in the deep shelf, resulting in a deeper mixed layer depth on the shelf.

2021). With warming intensifies, sea ice declines, and glacier melt accelerates (Shepherd *et al* 2018, Purich and Doddridge 2023). Research on the Cosmonaut Sea could provide more insights into future changes in the SO overturning circulation.

The Chl *a* distribution along the coastal section indicates that basal melting of the ice shelf supports the deeper survival of phytoplankton (figure 3). These deep-water phytoplankton may be adapted to low-light conditions. The flourishing of phytoplankton under Antarctic sea ice is partly due to their adaption to low light (Horvat *et al* 2022). Previous studies have pointed out that microalgae can adapt to low irradiance conditions by expanding light-harvesting complexes and adjusting pigment composition (Van Leeuwe and Stefels 2007, Van Leeuwe *et al* 2018). Dissolved iron from basal melting of the ice shelf may enhance phytoplankton growth in low-light environments. Additionally, a deeper MLD may bring more nutrients, particularly iron, from the deep sea, leading to an increase in Chl *a*. In early spring, the timing of phytoplankton blooms is controlled by light availability (Perovich 1990), while the supply of iron limits phytoplanton biomass and community composition later in the SO (Boyd *et al* 2000). Our results support the survival of phytoplankton in nutrients (iron)-rich, low-light depths during the study period (from 27 January to 11 March).

4.2. Effects of SIM, MW, and WW on phytoplankton biomass

Iron is considered the primary limiting nutrient regulating phytoplankton growth in the SO (Wang *et al* 2020). SIM and GMW are important sources of dissolved iron for phytoplankton growth in the SO (Lannuzel *et al* 2010, Herraiz-Borreguero *et al* 2016). McGillicuddy *et al* (2015) estimated the dissolved iron concentration in GMW to be 29 ± 21 nM based on measurements from Antarctic glacier ice cores, while St-Laurent *et al* (2017) estimated a value of 20 nM. Measured dissolved iron concentrations in SIM range from 1.1 to 30.2 nM in West Antarctica and from 0.7 to 36.8 nM in East Antarctica (Lannuzel *et al* 2016). The physical processes that transport iron-rich subsurface water to the surface are mainly winter deep mixing and diapycnal diffusion (Tagliabue *et al* 2014). As WW is a remnant of the previous winter's mixed layer, it more or less reflects the summer status of iron availability to upper phytoplankton. Phytoplankton growth typically peaks when the surface mixed layer is stratified (Sambrotto *et al* 2003). In addition to providing iron, surface input of freshwater and WW also promote phytoplankton growth by increasing water stability (Zhang *et al* 2014, 2019, Behera *et al* 2020, Sabu *et al* 2020).

As mentioned in section 4.1, MW did not significantly enhance water stability in the Cosmonaut Sea, and no significant positive correlation was observed between Chl *a* and MLD. To understand the potential mechanisms by which freshwater components promote phytoplankton growth, we performed a principal component analysis to examine the relationships among SIM, MW, WW, MLD, and total Chl *a* above 200 m. Our results indicate that the first two dimensions (Dims) explain 77.8% of the total variation, with Dim1 explaining 65.8% and Dim2 explaining 12%. All variables contributed to the formation of Dim1. MW, MLD and total Chl *a* negatively impacted the loading of Dim2, whereas SIM and WW had a positive impact (figure S7). As previous discussed, in the Cosmonaut Sea, SIM, MW, WW and MLD enhanced iron input, but only SIM and WW increased water stability. These relationships suggest that Dim1 is primarily associated with iron supply, while Dim2 is related to water stability. Thus, the vertical stability of seawater has minimal impact on phytoplankton growth in the Cosmonaut Sea, and the primary mechanism by which freshwater and WW promote phytoplankton growth is through the supply of dissolved iron.

4.3. Effects of SIM and MW on phytoplankton composition

As illustrated in table 2 and figure S5, SIM and MW favor the growth of larger phytoplankton (micro-phytoplankton and nano-phytoplankton). These observations are consistent with results reported in the literature (Gervais *et al* 2002). Both natural iron fertilization and controlled shipboard iron addition experiments have demonstrated that adding iron can boost phytoplankton growth rates and shift community structure towards larger diatoms (Boyd *et al* 2000, Gervais *et al* 2002, Xu *et al* 2014). Nevertheless, no significant correlation was identified between freshwater and the percentage of micro-phytoplankton (figures 4(a) and (b)). These conclusions are not contradictory because the growth-promoting effects of freshwater on different size Chl *a* vary under different conditions. Additionally, micro-Chl *a* contained different phytoplankton species at different stations, and the effects of freshwater on each species also varied. Consequently, the proportion of micro-phytoplankton from total phytoplankton may be high even when their biomass is low. This indicates that SIM and MW were not the dominant factors in the proportion of different size Chl *a* in the Cosmonaut Sea.

The SIM content exhibited a positive correlation with the proportion of Bacillariophyta, while showing a negative correlation with the proportion of *Phaeocystis sp.* (figures 4(c) and (d)), consistent with results reported in the literature (Moreau *et al* 2019). However, the MW content did not show any significant correlation with the proportion of Bacillariophyta and *Phaeocystis sp.* (figures 4(e) and (f)). Previous studies have shown that higher water stability favors

the growth of diatoms (Arrigo *et al* 1999). One study reported that diatoms constituted more than 70% of the phytoplankton population only at stations where the MLD was less than 20 m in the Ross Sea (Arrigo *et al* 2000). However, MW from basal melting of the ice shelf resulted in a deeper MLD in the Cosmonaut Sea. Consequently, MW did not significantly increase the proportion of Bacillariophyta, although both SIM and MW could supply iron. Therefore, changes in sea ice could significantly affect the phytoplankton community in the Cosmonaut Sea under climate change.

5. Conclusions

In the Cosmonaut Sea, the SIM content is higher at the edge of the continental shelf, indicating increased sea ice melting and reduced northward sea ice export. The MW content is higher in coastal waters, significantly contributed by basal melting of ice shelves. The low sea ice export and basal melting of ice shelves lead to a deeper MLD and a greater phytoplankton survival depth on the shelf. SIM, MW and WW are important factors promoting phytoplankton growth. The relationship between SIM, MW, WW, MLD, and Chl *a* suggests that the primary mechanism stimulating phytoplankton growth is not water stability but the nutrients (dissolved iron) provided by freshwater. Freshwater may be more conducive to the growth of larger phytoplankton, but no significant correlation was identified between freshwater and the percentage of micro-phytoplankton, indicating that freshwater was not the dominant factor in the proportion of different size Chl *a*. SIM significantly promoted the proportion of Bacillariophyta and reduced the proportion of *Phaeocystis sp.*

Data availability statements

Data representation was performed with ocean data view (Schlitzer, R., Ocean Data View, http://odv.awi.de). Calculations by SIAR model were carried out with the statistical program R (https://cloud.r-project.org, v. 4.1.1).

The data that support the findings of this study are openly available at the following URL/DOI: https://doi.org/10.5281/zenodo.13118418.

Acknowledgment

The authors would like to thank the captains and crews of the R/V Xuelong 2 for their assistance in sampling. This work was supported by Polar Research Institute of China (IRASCC 02-01-01 and IRASCC 01-01-02C), and National Natural Science Foundation of China (41721005).

ORCID iDs

Qianqian Qi https://orcid.org/0009-0000-1706-0796
Shunan Cao https://orcid.org/0000-0002-3264-851X
Min Chen https://orcid.org/0000-0003-0369-694X

References

Anderson R, Ali S, Bradtmiller L, Nielsen S, Fleisher M, Anderson B and Burckle L 2009 Wind-driven upwelling in the Southern Ocean and the deglacial rise in atmospheric CO_2 *Science* **323** 1443–8
Arrigo K R, DiTullio G R, Dunbar R B, Robinson D H, VanWoert M, Worthen D L and Lizotte M P 2000 Phytoplankton taxonomic variability in nutrient utilization and primary production in the Ross Sea *J. Geophys. Res. Oceans* **105** 8827–46
Arrigo K R, Robinson D H, Worthen D L, Dunbar R B, DiTullio G R, VanWoert M and Lizotte M P 1999 Phytoplankton community structure and the drawdown of nutrients and CO_2 in the Southern Ocean *Science* **283** 365–7
Auger M, Morrow R, Kestenare E, Sallée J-B and Cowley R 2021 Southern Ocean *in-situ* temperature trends over 25 years emerge from interannual variability *Nat. Commun.* **12** 514
Banwell A 2017 Ice-shelf stability questioned *Nature* **544** 306–7
Behera N, Swain D and Sil S 2020 Effect of Antarctic sea ice on chlorophyll concentration in the Southern Ocean *Deep-Sea Res. II: Top. Stud. Oceanogr.* **178** 104853
Biddle L C, Loose B and Heywood K J 2019 Upper ocean distribution of glacial meltwater in the Amundsen Sea, Antarctica *J. Geophys. Res. Oceans* **124** 6854–70
Boyd P W, Watson A J, Law C S, Abraham E R, Trull T, Murdoch R, Bakker D C, Bowie A R, Buesseler K and Chang H 2000 A mesoscale phytoplankton bloom in the polar Southern Ocean stimulated by iron fertilization *Nature* **407** 695–702
Brown P J, Meredith M P, Jullion L, Naveira Garabato A, Torres-Valdés S, Holland P, Leng M J and Venables H 2014 Freshwater fluxes in the Weddell Gyre: results from $\delta^{18}O$ *Phil. Trans. R. Soc.* A **372** 20130298
Evans J St B T, Handley S J, Perham N, Over D E and Thompson V A 2000 Frequency versus probability formats in statistical word problems *Cognition* **77** 197–213
Gervais F, Riebesell U and Gorbunov M Y 2002 Changes in primary productivity and chlorophyll a in response to iron fertilization in the Southern Polar Frontal Zone *Limnol. Oceanogr.* **47** 1324–35
Haumann F A, Gruber N, Münnich M, Frenger I and Kern S 2016 Sea-ice transport driving Southern Ocean salinity and its recent trends *Nature* **537** 89–92
Herraiz-Borreguero L, Lannuzel D, van der Merwe P, Treverrow A and Pedro J 2016 Large flux of iron from the Amery Ice Shelf marine ice to Prydz Bay, East Antarctica *J. Geophys. Res. Oceans* **121** 6009–20
Horvat C, Bisson K, Seabrook S, Cristi A and Matthes L C 2022 Evidence of phytoplankton blooms under Antarctic sea ice *Front. Mar. Sci.* **9** 942799
Hyder P, Edwards J M, Allan R P, Hewitt H T, Bracegirdle T J, Gregory J M, Wood R A, Meijers A J, Mulcahy J and Field P 2018 Critical Southern Ocean climate model biases traced to atmospheric model cloud errors *Nat. Commun.* **9** 3625
Jeon M H, Jung J, Park M O, Aoki S, Kim T-W and Kim S-K 2021 Tracing circumpolar deep water and glacial meltwater using humic-like fluorescent dissolved organic matter in the Amundsen Sea, Antarctica *Mar. Chem.* **235** 104008

Jia R, Chen M, Pan H, Zeng J, Zhu J, Liu X, Zheng M and Qiu Y 2022 Freshwater components track the export of dense shelf water from Prydz Bay, Antarctica *Deep-Sea Res. II: Top. Stud. Oceanogr.* **196** 105023

Landschützer P, Gruber N, Haumann F A, Rödenbeck C, Bakker D C, Van Heuven S, Hoppema M, Metzl N, Sweeney C and Takahashi T 2015 The reinvigoration of the Southern Ocean carbon sink *Science* **349** 1221–4

Lannuzel D, Schoemann V, De Jong J, Pasquer B, Van der Merwe P, Masson F, Tison J L and Bowie A 2010 Distribution of dissolved iron in Antarctic sea ice: spatial, seasonal, and inter-annual variability *J. Geophys. Res.* **115** G03022

Lannuzel D, Vancoppenolle M, van Der Merwe P, De Jong J, Meiners K M, Grotti M, Nishioka J and Schoemann V 2016 Iron in sea ice: review and new insights *Elementa Sci. Anthropocene* **4** 000130

Lenaerts J, Lhermitte S, Drews R, Ligtenberg S, Berger S, Helm V, Smeets C, Broeke M V D, Van De Berg W J and Van Meijgaard E 2017 Meltwater produced by wind–albedo interaction stored in an East Antarctic ice shelf *Nat. Clim. Change* **7** 58–62

Li Y, Zhao J, Li D, Pan J, He J, Hu J, Yu P, Zhang C, Yang X and Zhang H 2024 Factors controlling the phytoplankton crops, taxonomic composition, and particulate organic carbon stocks in the Cosmonaut Sea, East Antarctica *J. Ocean. Limnol.* (https://doi.org/10.1007/s00343-024-3198-6)

McGillicuddy D Jr, Sedwick P N, Dinniman M S, Arrigo K, Bibby T, Greenan B, Hofmann E E, Klinck J M, Smith W O Jr and Mack S 2015 Iron supply and demand in an Antarctic shelf ecosystem *Geophys. Res. Lett.* **42** 8088–97

Meijers A, Klocker A, Bindoff N, Williams G and Marsland S 2010 The circulation and water masses of the Antarctic shelf and continental slope between 30 and 80 °E *Deep-Sea Res. II: Top. Stud. Oceanogr.* **57** 723–37

Meredith M P, Wallace M I, Stammerjohn S E, Renfrew I A, Clarke A, Venables H J, Shoosmith D R, Souster T and Leng M J 2010 Changes in the freshwater composition of the upper ocean west of the Antarctic Peninsula during the first decade of the 21st century *Prog. Oceanogr.* **87** 127–43

Minowa M, Sugiyama S, Ito M, Yamane S and Aoki S 2021 Thermohaline structure and circulation beneath the Langhovde Glacier ice shelf in East Antarctica *Nat. Commun.* **12** 4209

Moore K, Fayek M, Lemes M, Rysgaard S and Holländer H M 2017 Fractionation of hydrogen and oxygen in artificial sea ice with corrections for salinity for determining meteorological water content in bulk ice samples *Cold Reg. Sci. Technol.* **142** 93–99

Moreau S, Lannuzel D, Janssens J, Arroyo M, Corkill M, Cougnon E, Genovese C, Legresy B, Lenton A and Puigcorbe V 2019 Sea ice meltwater and circumpolar deep water drive contrasting productivity in three Antarctic polynyas *J. Geophys. Res. Oceans* **124** 2943–68

Morgan V 1972 Oxygen isotope evidence for bottom freezing on the Amery Ice Shelf *Nature* **238** 393–4

Morgan V 1982 Antarctic ice sheet surface oxygen isotope values *J. Glaciol.* **28** 315–23

Orsi A H, Whitworth T III and Nowlin W D Jr 1995 On the meridional extent and fronts of the Antarctic Circumpolar Current *Deep-Sea Res. I: Oceanogr. Res. Pap.* **42** 641–73

Parnell A C, Inger R, Bearhop S and Jackson A L 2010 Source partitioning using stable isotopes: coping with too much variation *PLoS One* **5** e9672

Perovich D K 1990 Theoretical estimates of light reflection and transmission by spatially complex and temporally varying sea ice covers *J. Geophys. Res. Oceans* **95** 9557–67

Pritchard H, Ligtenberg S R, Fricker H A, Vaughan D G, van den Broeke M R and Padman L 2012 Antarctic ice-sheet loss driven by basal melting of ice shelves *Nature* **484** 502–505

Purich A and Doddridge E W 2023 Record low Antarctic sea ice coverage indicates a new sea ice state *Commun. Earth Environ.* **4**

Qi Q 2024 Diverse impacts of sea ice and ice shelf melting on phytoplankton communities in the Cosmonaut Sea, East Antarctica [Dataset] *Zenodo* (https://doi.org/10.5281/zenodo.13118418)

Rignot E, Velicogna I, van den Broeke M R, Monaghan A and Lenaerts J T 2011 Acceleration of the contribution of the Greenland and Antarctic ice sheets to sea level rise *Geophys. Res. Lett.* **38** L05503

Rintoul S R 2018 The global influence of localized dynamics in the Southern Ocean *Nature* **558** 209–18

Sabine C L, Feely R A, Gruber N, Key R M, Lee K, Bullister J L, Wanninkhof R, Wong C, Wallace D W and Tilbrook B 2004 The oceanic sink for anthropogenic CO_2 *Science* **305** 367–71

Sabu P, Libera S A, Chacko R, Anilkumar N, Subeesh M and Thomas A P 2020 Winter water variability in the Indian Ocean sector of Southern Ocean during austral summer *Deep-Sea Res. II: Top. Stud. Oceanogr.* **178** 104852

Sambrotto R N, Matsuda A, Vaillancourt R, Brown M, Langdon C, Jacobs S S and Measures C 2003 Summer plankton production and nutrient consumption patterns in the Mertz Glacier region of East Antarctica *Deep-Sea Res. II: Top. Stud. Oceanogr.* **50** 1393–414

Shepherd A, Fricker H A and Farrell S L 2018 Trends and connections across the Antarctic cryosphere *Nature* **558** 223–32

Shields A R and Smith W O 2009 Size-fractionated photosynthesis/irradiance relationships during *Phaeocystis antarctica*-dominated blooms in the Ross Sea, Antarctica *J. Plankton Res.* **31** 701–12

Silvano A, Rintoul S R, Peña-Molino B, Hobbs W R, van Wijk E, Aoki S, Tamura T and Williams G D 2018 Freshening by glacial meltwater enhances melting of ice shelves and reduces formation of Antarctic Bottom Water *Sci. Adv.* **4** eaap9467

Smith W O Jr, Marra J, Hiscock M R and Barber R T 2000 The seasonal cycle of phytoplankton biomass and primary productivity in the Ross Sea, Antarctica *Deep-Sea Res. II: Top. Stud. Oceanogr.* **47** 3119–40

St-Laurent P, Yager P, Sherrell R, Stammerjohn S and Dinniman M 2017 Pathways and supply of dissolved iron in the Amundsen Sea (Antarctica) *J. Geophys. Res. Oceans* **122** 7135–62

Tagliabue A, Sallée J-B, Bowie A R, Lévy M, Swart S and Boyd P W 2014 Surface-water iron supplies in the Southern Ocean sustained by deep winter mixing *Nat. Geosci.* **7** 314–20

Tamura T P, Nomura D, Hirano D, Tamura T, Kiuchi M, Hashida G, Makabe R, Ono K, Ushio S and Yamazaki K 2023 Impacts of basal melting of the Totten Ice Shelf and biological productivity on marine biogeochemical components in Sabrina Coast, East Antarctica *Global Biogeochem. Cycles* **37** e2022GB007510

Van Leeuwe M A, Tedesco L, Arrigo K R, Assmy P, Campbell K, Meiners K M, Rintala J-M, Selz V, Thomas D N and Stefels J 2018 Microalgal community structure and primary production in Arctic and Antarctic sea ice: a synthesis *Elem. Sci. Anth.* **6** 4

Van Leeuwe M and Stefels J 2007 Photosynthetic responses in *Phaeocystis antarctica* towards varying light and iron conditions *Biogeochemistry* **83** 61–70

Wang B, Chen M, Chen F, Jia R, Li X, Zheng M and Qiu Y 2020 Meteoric water promotes phytoplankton carbon fixation

and iron uptake off the eastern tip of the Antarctic Peninsula (eAP) *Prog. Oceanogr.* **185** 102347

Welschmeyer N A 1994 Fluorometric analysis of chlorophyll a in the presence of chlorophyll b and pheopigments *Limnol. Oceanogr.* **39** 1985–92

West N J, Landa M and Obernosterer I 2024 Differential association of key bacterial groups with diatoms and *Phaeocystis* spp. during spring blooms in the Southern Ocean *MicrobiolOpen* **13** e1428

Williams G, Herraiz-Borreguero L, Roquet F, Tamura T, Ohshima K, Fukamachi Y, Fraser A, Gao L, Chen H and McMahon C 2016 The suppression of Antarctic bottom water formation by melting ice shelves in Prydz Bay *Nat. Commun.* **7** 12577

Xu K, Fu F-X and Hutchins D A 2014 Comparative responses of two dominant Antarctic phytoplankton taxa to interactions between ocean acidification, warming, irradiance, and iron availability *Limnol. Oceanogr.* **59** 1919–31

Yamazaki K, Aoki S, Katsumata K, Hirano D and Nakayama Y 2021 Multidecadal poleward shift of the southern boundary of the Antarctic Circumpolar Current off East Antarctica *Sci. Adv.* **7** eabf8755

Yamazaki K, Aoki S, Shimada K, Kobayashi T and Kitade Y 2020 Structure of the subpolar gyre in the Australian-Antarctic Basin derived from Argo floats *J. Geophys. Res. Oceans* **125** e2019JC015406

Zhang R, Ma Q, Chen M, Zheng M, Cao J and Qiu Y 2019 Nitrogen uptake regime regulated by ice melting during austral summer in the Prydz Bay, Antarctica *Acta Oceanol. Sin.* **38** 1–7

Zhang R, Zheng M, Chen M, Ma Q, Cao J and Qiu Y 2014 An isotopic perspective on the correlation of surface ocean carbon dynamics and sea ice melting in Prydz Bay (Antarctica) during austral summer *Deep-Sea Res. I: Oceanogr. Res. Pap.* **83** 24–33